

# Exact zero modes in the interacting Majorana X- and Y-junctions

Rik Mulder, Bowy M. La Rivière,\* and Natalia Chepiga

Kavli Institute of Nanoscience, Delft University of Technology, Lorentzweg 1, 2628CJ Delft, The Netherlands

(Dated: June 15, 2025)

We report the appearance of exact zero modes in junctions of interacting Majorana wires. We consider two, three and four short Majorana chains coupled to each other at one edge and forming a longer chain with an impurity bond, Y- and X- junctions correspondingly. The exact zero modes emerge as a result of incommensurate short-range correlations resulting from interacting Majorana fermions and manifest themselves as unavoided crossing of energy levels of in-gap states continuously tuned by hopping and interaction strength. For the Y- and X-junctions, we detect four in-gap states that are clearly visible below the bulk excitations. In the X-junction, the energy levels cross pairwise; in the Y-junction, the crossings happen simultaneously in all four levels. We argue that this peculiarity is a result of fractional degrees of freedom localized at the center of junctions with an odd number of arms, which mediate the interaction of the outer edge states. Furthermore, we show that zero modes in multiple-arm junctions can be effectively modeled by a single chain with a strong impurity bond.

## I. INTRODUCTION

Topological phases of matter have been at the forefront of condensed matter physics. In particular, Majorana fermions - particles that are their own antiparticles - have been of interest because they provide a foundational framework for fault tolerant quantum computing [1–3]. As noted by Kitaev [4], a chain of spinless fermions - an effective model of a  $p$ -wave superconductor - displays topologically non-trivial properties with a single "unpaired" zero-energy Majorana fermion localized at its edges. Interestingly, in non-interacting systems these zero modes affect the entire many-body spectrum and are therefore referred to as *strong* zero modes (SZM) - a term popularized by Fendley [5]. Observing signatures of these SZM has been the hallmark in various works over the past decades in a search to realize Majorana edge states in an experimental setup [6–12].

By definition Majorana fermions in the Kitaev chain are non-interacting. However, since fermions experience repulsion, a natural extension is to add interaction between them [13–19]. Such interacting Majorana chains have been studied in various contexts, including quantum phase transitions [19–23], and in the presence of quenched disorder [24–30] with a recent focus on many-body localization at high energy [31–35]. Several types of interaction have been considered in the literature, but here we focus on the translationally-invariant Hamiltonian with the simplest non-trivial interaction described by

$$\mathcal{H} = \sum_j it\gamma_j\gamma_{j+1} - g\gamma_j\gamma_{j+1}\gamma_{j+2}\gamma_{j+3}, \quad (1)$$

where  $\gamma_i$  are the typical Majorana fermionic operators satisfying  $\gamma_j^\dagger = \gamma_j$ ,  $\gamma_j^2 = 1$  and  $\{\gamma_i, \gamma_j\} = 2\delta_{ij}$ ;  $t$  is a

hopping amplitude and  $g$  is a coupling strength of the interaction term.

Contrary to the non-interacting case, no explicit and exact construction of SZM exist for this model or interacting chains in general [36–39] - the notable exception being the integrable XXZ chain [40]. However, the  $\mathbb{Z}_2$  phase dual to the topological trivial phase contains a large incommensurate region [19]. While this does not guarantee the presence of SZM, incommensurability allows one to fine-tune the system to the set of points where energy levels of the in-gap states cross each other resulting in *exact* zero modes (EZM) [12, 41–44].

The problem of Y- and multiple-chain junctions has a long history and attracted a lot of attention, in particular in the context of coupled superconducting wires [45–48] and the proposal for braiding of Majorana fermions based on the tri-junction [49]. Recent progress on Majorana corner states in second order topological superconductors [50–53] might eventually open new avenues to explore more complex junctions as well. The study of localized edge states in these systems, on the other hand, is very scarce and limited to the situations when the outer edge states are screened [54] or pushed far away from the junction [55]. Here we aim to fill this knowledge gap by studying Majorana edge states and in-gap states over moderate-sized Y- and X-junctions of interactive Kitaev chains described by Eq. (1) coupled at the edges. We show a sketch of each junction in Fig.1 including the junction of two chains that we use as a benchmark. The in-gap states are easily accessible numerically through exact diagonalization or by targeting excited states in the density matrix renormalization group (DMRG) algorithm [56].

In this paper we study the family of spin Hamiltonians, dual to the coupled interacting Kitaev chains, defined as

$$\mathcal{H}^{(n)} = \sum_i^n \sum_j (J\sigma_{i,j}^x\sigma_{i,j+1}^x - h\sigma_{i,j}^z + g\sigma_{i,j}^z\sigma_{i,j+1}^z + g\sigma_{i,j}^x\sigma_{i,j+2}^x) + \mathcal{H}_{\text{coupling}}(\alpha), \quad (2)$$

\* Contact author: b.m.lariviere@tudelft.nl

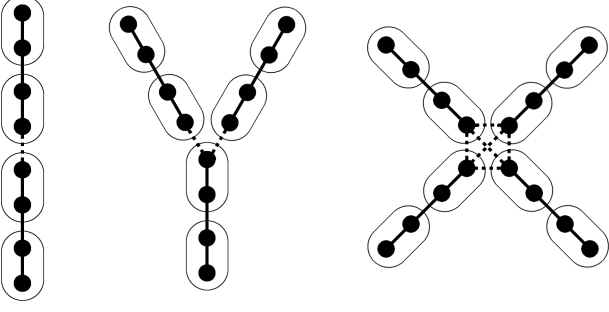


FIG. 1. Sketches of the structures considered here (from left to right); two coupled Majorana chains, three coupled in the Y-junction, and four chains coupled in the X-junction. Dotted lines denote which chains couple to each other.

where  $\sigma_{i,j}^x$  and  $\sigma_{i,j}^z$  are Pauli matrices acting on site  $j$  in chain  $i$  and  $n$  is the number of chains. Here we use  $h$  and  $J$  notations of the transverse field Ising model  $t(2j) = h$  and  $t(2j+1) = -J$  explicitly allowing the alternation in the Majorana hopping term when  $h \neq J$ . The coupling term  $\mathcal{H}_{\text{coupling}}(\alpha)$  is a function of the coupling strength  $\alpha$  and depends on the number of chains coupled (we define the coupling for each junction in more detail in the corresponding sections). Note, the first sum over  $j$  simply describes the spin-Hamiltonian obtained by applying the Jordan-Wigner transformation on the interacting Kitaev chain described in Eq. 1. We only consider chains of an even number of Majorana fermions and spins. We study oscillations in the ground state energies by tuning the system into the incommensurate  $\mathbb{Z}_2$  ordered phase located at  $|h| < 1$  and  $0 < g \lesssim 0.4$  [19]. For more information on the mapping and how we extract the low-energy spectrum of the Hamiltonian, we refer to Appendix A

The rest of the paper is structured as follows. In Sec. II we benchmark our method with the simplest case of two coupled chains. We present numerical evidences of the exact zero modes in the Y-junction in Sec. III. In Sec. IV we study exact zero modes appearing in X-junction. We conclude our results and put them into perspective in Sec. V.

## II. TWO COUPLED CHAINS

We start our analysis with two chains with the two ends coupled to each other. Equivalently, one can consider this system as a long chain with a single impurity bond. The junction of two Majorana chains has been considered recently in Ref.[57] in which the coupling constants were different on the two sides of the junction. Here we couple two identical Majorana chains. The coupling term consists of all two and four Majorana operators that overlap

with the junction:

$$\begin{aligned} \mathcal{H}_{\text{coupling}}(\alpha) &= \mathcal{H}^{(i,j)} \\ &\equiv \alpha \left[ it\gamma_{i,N_i}\gamma_{j,N_j} - g(\gamma_{i,N_i-2}\gamma_{i,N_i-1}\gamma_{i,N_i}\gamma_{j,N_j} \right. \\ &\quad + \gamma_{i,N_i-1}\gamma_{i,N_i}\gamma_{j,N_j-1}\gamma_{j,N_j} \\ &\quad \left. + \gamma_{i,N_i}\gamma_{j,N_j-2}\gamma_{j,N_j-1}\gamma_{j,N_j} \right]. \end{aligned} \quad (3)$$

Through the Jordan-Wigner transformation, we obtain

$$\begin{aligned} \mathcal{H}^{(i,j)} &= \alpha g \sigma_{i,\tilde{N}_i}^z \sigma_{j,\tilde{N}_j}^z \\ &\quad + \alpha i \left( J \sigma_{i,\tilde{N}_i}^x \sigma_{j,\tilde{N}_j}^x + g \sigma_{i,\tilde{N}_i-1}^x \sigma_{j,\tilde{N}_j}^x \right. \\ &\quad \left. + g \sigma_{i,\tilde{N}_i}^x \sigma_{j,\tilde{N}_j-1}^x \right) \prod_{i < m \leq j, k=1}^{k=\tilde{N}_m} \sigma_{m,k}^z, \end{aligned} \quad (4)$$

where  $i$  and  $j$  label two chains, here simply  $i = 1$  and  $j = 2$ ,  $N_i$  is the number of Majorana fermions in chain  $i$  and  $\tilde{N}_i = N_i/2$  denotes the number of spins. Despite looking non-Hermitian, the Hamiltonian is in fact Hermitian due to one of the  $\sigma_z$ -operators in the  $\sigma_z$ -string acting on the same site as the  $\sigma_x$ -operator in chain  $j$ . The string of  $\sigma^z$  operators is a result of ordering of the two chains (see final paragraph of Appendix A for more information). In Fig.2(a) we show the four lowest energies for  $N_i = N_j = 12$  as a function of the coupling strength  $\alpha$ . For visual clarity, we center the data around their average. The levels are labeled by the corresponding parity of the state, computed as:

$$P = \prod_{i=1}^n \prod_{j=1}^{\tilde{N}_i} \sigma_{i,j}^z, \quad (5)$$

associated with each energy, where the product is taken over all spins in all chains. We observe that when the two chains are uncoupled, the ground and second excited state are both unique and have  $P = 1$ , while the first excited state is double degenerate with  $P = -1$ . When we couple the two chains this degeneracy is lost and two states with opposite parity pair up and form in-gap states while the other two become excited states. From now on we will refer to these as *parity pairs* and *bulk* states respectively.

For the two ground states we show their dependence on the magnetic field  $h$  - effective parameter that allows to tune the coupling between the edge states [19] - in Fig.2(b) for when the chains are weakly coupled, i.e.  $\alpha = 0.015$ . Furthermore, we also show the two ground state energies of a single interacting Kitaev chain of  $N = 12$  Majorana fermions on top. The two coupled chains show clear oscillations. Interestingly, even for two very weakly coupled chains EZM appear. However, unlike the normal interacting Kitaev chain, the interval in which the negative parity sector is the ground state is very small in comparison to the positive parity sector. The location of the vanishing parity gap of the single

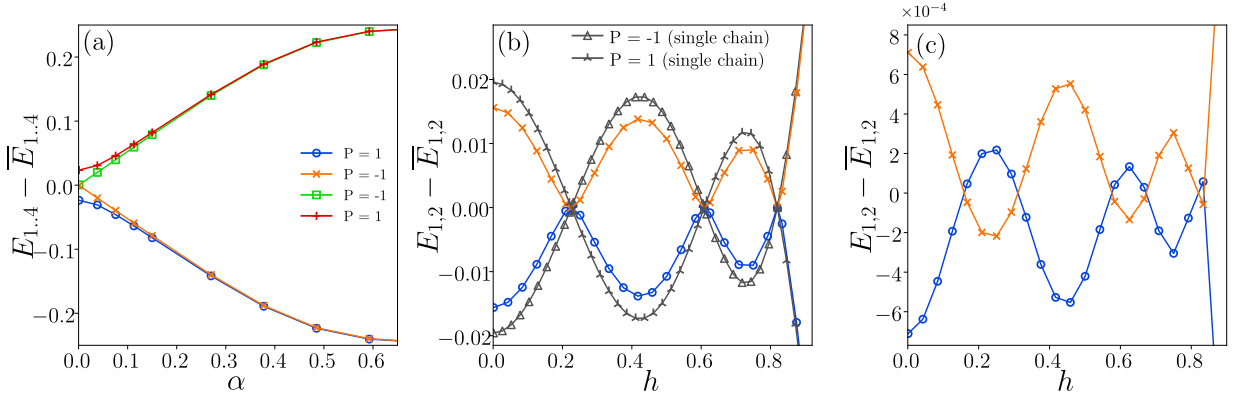


FIG. 2. Numerical results of the energy spectrum of two coupled chains each with  $N = 12$  Majorana fermions. Simulations were done for  $g = 0.2$ . (a) Four lowest eigenenergies centered around their average of the four as a function of the coupling strength  $\alpha$ . Chains are uncoupled for  $\alpha = 0$ . Colours denote the parity of the entire chain. When chains are coupled, two states with opposite parity become part of the ground state spectrum. Data shown for  $h = 0.735$ . (b) Ground state energy as a function of the magnetic field  $h$  for small coupling strength  $\alpha = 0.015$ . We also show the ground state energy for a single interacting Kitaev chain of  $N = 12$  Majorana fermions (gray curves). Data is centered around the average of the ground states. Note that as soon as  $\alpha > 0$  exact zero modes appear, but for small  $\alpha$  the intervals where negative parity state is a ground-state are much shorter compare to the intervals where the ground-state has  $P = 1$ . (c) Same as in (b) but for a coupling strength  $\alpha = 0.6$ .

chain matches the location where the parity gap is the smallest for the coupled chains.

When increasing the coupling up to  $\alpha = 0.6$ , Fig.2(c), there are clear EZM present in the ground state. The number of these EZM matches that of a single chain of  $N = 24$  [19]. Intuitively, two energy levels that were only touching at  $\alpha = 0.015$  in Fig.2(b) now, for a finite  $\alpha$ , overlap resulting to exact energy crossings but with an alternating amplitude that will naturally vanish upon approaching a single-chain limit  $\alpha \rightarrow 1$  where symmetry between even and odd parity sectors will be restored.

### III. THE Y-JUNCTION: THREE COUPLED CHAINS

Let us now consider the case when three chains are coupled together forming a Y-junction. The full three-site coupling term is described by

$$\mathcal{H}_{\text{coupling}}(\alpha) = \left( \sum_{i=1}^2 \sum_{j>i}^3 \mathcal{H}^{(i,j)} \right) + \mathcal{H}^{(1,2,3)}, \quad (6)$$

where the first terms in the brackets describes all possible two chain couplings and we define

$$\begin{aligned} \mathcal{H}^{(i,j,k)} \equiv & -g\alpha^2 \left( \gamma_{i,N_i-1} \gamma_{i,N_i} \gamma_{j,N_j} \gamma_{k,N_k} \right. \\ & + \gamma_{i,N_i} \gamma_{j,N_j-1} \gamma_{j,N_j} \gamma_{k,N_k} \\ & \left. + \gamma_{i,N_i} \gamma_{j,N_j} \gamma_{k,N_k-1} \gamma_{k,N_k} \right), \end{aligned} \quad (7)$$

which in terms of spin-operator can be written as

$$\begin{aligned} \mathcal{H}^{(i,j,k)} = & g\alpha^2 i \left( \sigma_{i,\tilde{N}_i}^z \sigma_{j,\tilde{N}_j}^x \sigma_{k,\tilde{N}_k}^x \prod_{j<m\leq k, l=1}^{l=\tilde{N}_m} \sigma_{m,l}^z \right. \\ & + \sigma_{i,\tilde{N}_i}^x \sigma_{j,\tilde{N}_j}^z \sigma_{k,\tilde{N}_k}^x \prod_{i<m\leq k, l=1}^{l=\tilde{N}_m} \sigma_{m,l}^z \\ & \left. + \sigma_{i,\tilde{N}_i}^x \sigma_{j,\tilde{N}_j}^x \sigma_{k,\tilde{N}_k}^z \prod_{i<m\leq j, l=1}^{l=\tilde{N}_m} \sigma_{m,l}^z \right) \end{aligned} \quad (8)$$

as the term that couples three chains labeled  $i$ ,  $j$  and  $k$  with each other. Note, the factor  $\alpha^2$  comes from the fermionic Majorana operators crossing the gap between chains twice. For three chains of  $N = 12$  Majorana fermions each, we computed the energy spectrum, of which we plot the eight smallest as a function of the coupling strength  $\alpha$  in Fig.3(a). At  $\alpha = 0$  the degenerate sets of excitations come in triplets instead of doublets for a single chains, a direct consequence of having three arms in a junction. So, the ground state corresponds to a state with all three arms of a junction being in the parity sector  $P = 1$ , the first three-fold degenerate excitation corresponds to a state where two arms have parity  $+1$  and one arm has a parity  $-1$ , resulting in the total parity  $P = -1$ ; the next set of three-fold degenerate states is the one with two arms with parity  $-1$  and one with parity  $+1$ , so the overall parity is  $P = 1$  again; and finally, the eight in-gap state, highest in energy corresponds to all three arms being in the parity sector  $-1$ . As soon as  $\alpha > 0$  four out of the eight states become bulk excitations and the remaining four states form two pairs of in-gap states.

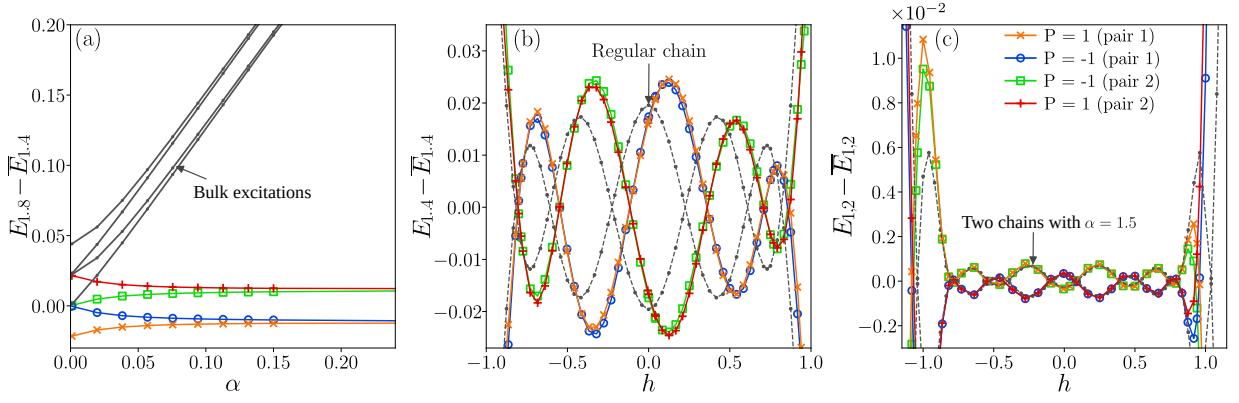


FIG. 3. Energy spectrum of three interactive Kitaev chains, each containing  $N = 12$  Majorana fermions, coupled by Eq. 6 in a Y-junction geometry for  $g = 0.2$ . (a) Eight lowest eigenenergies, centered around the average of the lowest four, as a function of the coupling strength  $\alpha$  and a fixed magnetic field  $h = 0.53$ . Four states become part of the ground state spectrum and group up into two pairs of opposite parity. Other states are greyed out and denote bulk states, i.e. no Majorana edge states. (b) Ground state quartet as a function of  $h$  at  $\alpha = 1$  centered average of the four states. Parity pairs show a vanishing energy gap between them when varying  $h$ . The similarity with a single interacting Kitaev chain of  $N = 12$  Majorana fermions (grey curve) is remarkable. (c) Same data as in (b) but centered around the average of each parity pair. Additionally, we show two chains of  $N = 12$  Majorana fermions each coupled with a strength  $\alpha = 1.5$ , which shows remarkable similarities to the ground state pairs.

In Fig.3(b) we show the dependence of the ground state spectrum on the magnetic field  $h$  for a fixed  $\alpha = 1$ . Again, for clarity we center the data around the average of the four energy levels. Similar to the previous case we detect exact level crossings with a vanishing energy gap. Note, it is not the parity gap that is vanishing but the energy gap between the two parity pairs, in other words, all four states are degenerate at the points of exact zero modes [58]. As we will see in the next section, this is a distinct property of a Y-junction, or, more precisely, of a junction with odd number of arms. In these case the odd number of zero modes in the center of a junction cannot annihilate but remain as an uncoupled Majorana zero mode mediating the interaction with outer edges of the junction.

We also show as a reference (grey lines in Fig.3(b)) the two ground states of a single interacting Kitaev chain of  $N = 12$  Majorana fermions - the same length as an arm in the Y-junction. Quite fascinating, both these show nearly the same oscillations with the same number of EZM, albeit occurring at a shifted location.

In Fig.3(c) we plot the same data as in the panel (b) but now centered around the average of each parity pair. There is a stark symmetry present: the same parity sectors of the two parity pairs completely mirror each other. Furthermore, a symmetry around  $h = 0$  appears that holds till the approximate boundary of the incommensurate region. Strikingly, the oscillations nearly perfectly match those of two chains of  $N = 12$  Majorana fermions each coupled by a strength  $\alpha = 1.5$ . Intuitively, one can argue that in the Y-junction each arm is coupled to two other arms, so when comparing with two coupled chains it is natural to expect  $\alpha > 1$ .

In addition we show in Fig.4(a) the energy dependence

on the four-fermion coupling strength  $g$  for a fixed  $h = 1$  and  $\alpha = 1$ ; the results are centered around the average of the four in-gap states. Similar to the single interacting chain [19], we see a clear present of EZM appearing upon tuning the coupling constant  $g$ . However, while the energy of the two states in a parity pair match well for small  $g$ , large values of  $g$  destroys this similarity, resulting in a sequence of pair-wise energy crossings.

We show the same data a semi-log scale in Fig.4(b), such that the exact zero modes near the disorder point are more visible. Rather interestingly, the similarity with the two chains coupled with  $\alpha \approx 1.5$  still holds, although the location of the EZM slightly differs from that of the Y-junction, in particular for larger  $g$ .

#### IV. THE X-JUNCTION: FOUR COUPLED CHAINS

Finally, let us consider the X-junction in which we couple four chains with each other. The terms that couples the chains is given by

$$\mathcal{H}_{\text{coupling}}(\alpha) = \left( \sum_{i=1}^3 \sum_{j>i}^4 \mathcal{H}^{(i,j)} \right) + \left( \sum_{i=1}^2 \sum_{j>i}^3 \sum_{k>j}^4 \mathcal{H}^{(i,j,k)} \right) + \mathcal{H}^{(1,2,3,4)}, \quad (9)$$

where term in the first brackets describes all possible two chain couplings, the second all possible three chain couplings, and the third all possible four chain couplings.

plings, and the final term

$$\begin{aligned}\mathcal{H}^{(i,j,k,l)} &\equiv g\alpha^3 \gamma_{i,N_i} \gamma_{j,N_j} \gamma_{k,N_k} \gamma_{l,N_l} \\ &= g\alpha^3 \sigma_{i,\tilde{N}_i}^x \sigma_{j,\tilde{N}_j}^x \sigma_{k,\tilde{N}_k}^x \sigma_{l,\tilde{N}_l}^x \left( \prod_{i < m < k, l=1}^{l=\tilde{N}_l} \sigma_{m,l}^z \right) \\ &\quad \times \left( \prod_{k < m \leq l, l=1}^{l=\tilde{N}_l} \sigma_{m,l}^z \right)\end{aligned}\quad (10)$$

describes the coupling for four chains labeled  $i, j, k$  and  $l$ . The factor  $\alpha^3$  comes from the Majorana operators crossing the center of the junction three times. We computed the ground state spectrum for four chains of  $N = 10$  Majorana fermions each, of which we show the 16 smallest energies in Fig.5(a). At  $\alpha = 0$  there again is a unique

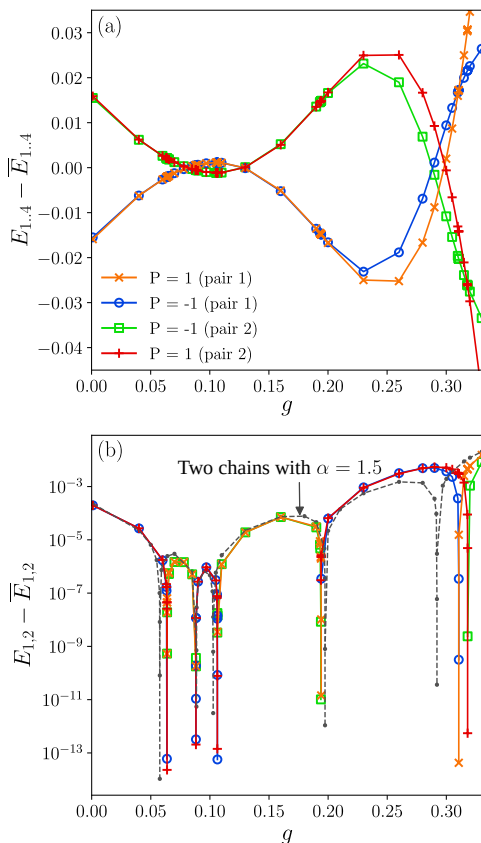


FIG. 4. Ground state energies as a function of the interaction strength  $g$  for three chains of  $N = 12$  Majorana fermions coupled in the Y-junction. We fix the magnetic field  $h = 0.53$  and coupling strength  $\alpha = 1$ . (a) Data centered around the average of the ground states. Ground states form two groups of two with opposite parity. Parity pairs are destroyed for increasing  $g$ . (b) Same data as in (a) but centered around the average of each parity pairs and shown in semi-log scale. We only show parts for which the relative energy is positive; dips indicate a vanishing parity gap. Grey dashed line corresponds to two chains of  $N = 12$  Majorana fermions each coupled by with  $\alpha = 1.5$ .

ground state with parity  $P = 1$ , but now the degenerate excitations appear in three quartets with one, two and three arms being in the negative parity sectors. The highest in energy in-gap state has parity  $-1$  on all legs, resulting in a total parity of the system  $P = 1$ . As soon as interaction in the junction is present and  $\alpha > 0$  the degeneracy of the quartet states is lifted and only four states remain as in-gap states for a finite  $\alpha$  while the other states become bulk excitations.

We show the dependence of this ground state spectrum on the magnetic field  $h$  in Fig.5(b) for four chains, each containing  $N = 10$  Majorana fermions. By contrast to the Y-junction, there is no unpaired Majorana degrees of freedom in the center of the junction, so the coupling of the outer edges is not mediated by the center. This results in a picture that looks qualitatively different from the previous case: the crossings do not happen in all four states at the same time, but pair-wise. This pair-wise structure can be seen clearly in Fig.5(c), where we present the same data as in the panel (b) but centered around the average of each parity pair. Quite remarkably, the ground state spectrum of two coupled chains resembles that of the X-junction, but now with the coupling strength  $\alpha = 2$ .

## V. CONCLUSION AND DISCUSSION

In this paper we report the appearance of exact zero modes in interacting Kitaev chains coupled in Y- and X-junctions. We focussed on topologically non-trivial phases with alternating hopping between even and odd pairs of Majorana sites and the simplest non-trivial interaction spanning four consecutive Majorana fermions. We studied the model numerically with exact diagonalization after mapping it to its dual spin-1/2 model.

We have found that out of the 8 (16) states of three (four) independent chains, only four states stay as an in-gap states when the chains are coupled into the Y- and X-junctions. These four states group into pairs with opposite parity, similar to that of the ground state of the single chain. Oscillations with a vanishing parity gap are present for each parity pair and, on top of that, the parity pairs show a vanishing energy gap as well.

Besides these similarities there are clear differences between the Y- and X-junctions though. Zero modes in Y-junction are mediated by a fractional degree of freedom located at the center of the junction. As the result, all four energy levels show a vanishing energy gap at the same point. By contrast, in the X-junction fractional degrees of freedom in the center of the junction are coupled together and all Majorana edge states are localized at the edges of a junction. This leads to a pair-wise crossing between in-gap states. We expect this effect to be a generic even-odd effect: in the junctions with odd number of sites interaction between edge states will always be mediated through fractional degrees of freedom located at the center of the junction. This suggests, in partic-

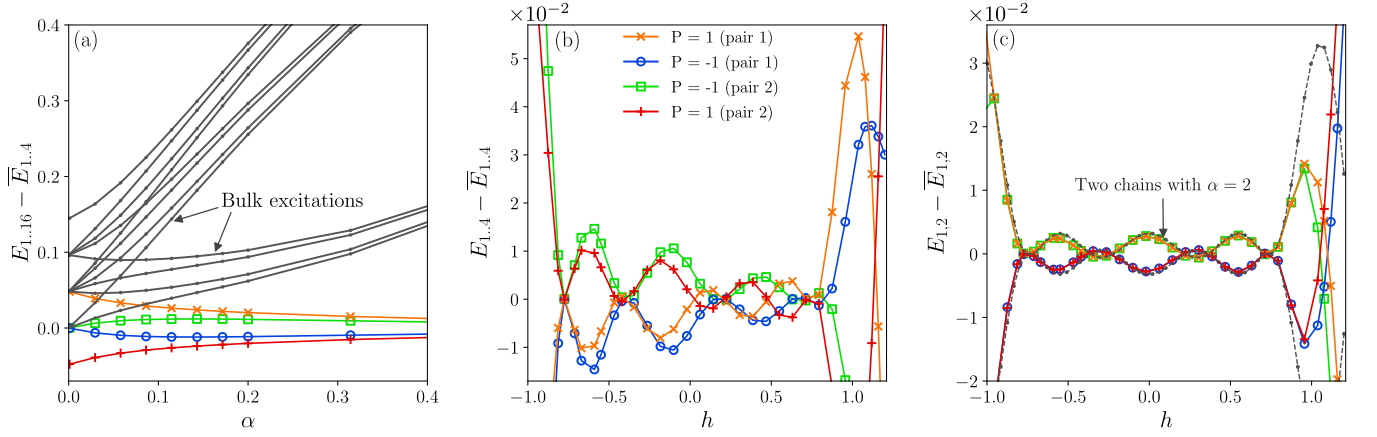


FIG. 5. Energy spectrum for four coupled Majorana chains of  $N = 10$  Majorana fermions each in the X-junction. Four fermions coupling is kept constant at  $g = 0.2$ . (a) 16 lowest energy levels as a function of the junction coupling strength  $\alpha$ . Data is centered around the average of the four lowest in-gap states. Magnetic field is kept constant at  $h = 0.7$ . (b) Four lowest in-gap states centered around its mean as a function of magnetic field  $h$  and for  $\alpha = 1$ . By contrast to the crossing all all four levels in the Y-junction presented in Fig.3(b), in X-junction the crossings happen pair-wise. (c) Same data as in the panel (b) but centered around the mean of each parity pair. Oscillations in the energy show a remarkable similarity with two chains coupled with a coupling strength  $\alpha = 2$  (grey line). We use the same color code for all three panels.

ular that centers of Y- and a generic odd-arm-junctions can be used as a single tuning knob to manipulate all outer edge states. This might be of particular interest, as the Y-junction has been used to realize braiding of Majorana fermions that requires the constant tuning of variables, such as the electrostatic potential, to move Majorana fermions around in the junction [49, 59–64].

Finally, there appears to be a strong similarity between the Y- and X-junction and a pair of coupled chains with an impurity bond being  $\alpha = 1.5$  and  $\alpha = 2$  respectively. These values likely depend on the number of arms added to the system: by doing so we indirectly increase the bonding strength between two chains opposite to each other in the junction. Determining whether these also depend on quantities such as the arm lengths is left out of scope for this study. Nonetheless, the resemblance between the Y- and X-junctions and two coupled chains suggests that a single chain with a strong impurity bond can be considered as an effective way to study exact zero modes within each parity pair in more complex multi-leg junctions.

## ACKNOWLEDGMENTS

NC thanks to Nicolas Laflorencie and Frederic Mila for insightful discussions and inspiring work on related subjects. This research has been supported by Delft Technology Fellowship. Numerical simulations have been performed with the Dutch national e-infrastructure with the support of the SURF Cooperative and at the DelftBlue HPC.

## Appendix A: Simulating coupled interactive Kitaev chains

### Mapping Majorana fermions to spins

Pauli operators can be mapped to Dirac fermions via the Jordan-Wigner transformation:

$$\begin{aligned}\sigma_j^z &= 1 - 2c_j^\dagger c_j, \\ \sigma_j^x &= K_j(c_j^\dagger + c_j), \\ \sigma_j^y &= iK_j(c_j^\dagger - c_j),\end{aligned}\tag{A1}$$

where  $K_j = \prod_{k=1}^{j-1} \sigma_k^z$ . For convenience, we rename all odd numbered Majorana operators  $\gamma_{2j+1} = a_j$  and all even numbered  $\gamma_{2j+1} = b_j$ . In terms of these Majorana

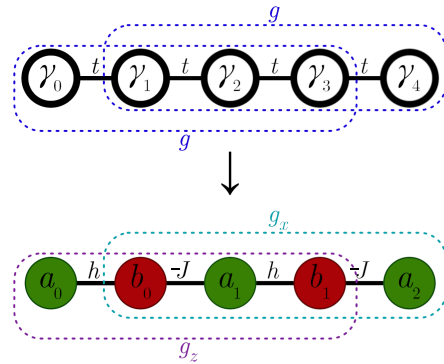


FIG. 6. Schematic picture of a Majorana chain in a representation where odd and even numbered are labeled as  $a$  and  $b$ . Hopping  $t$  and coupling  $g$  in the top part are shown in a spin-chain representation in the bottom chain.



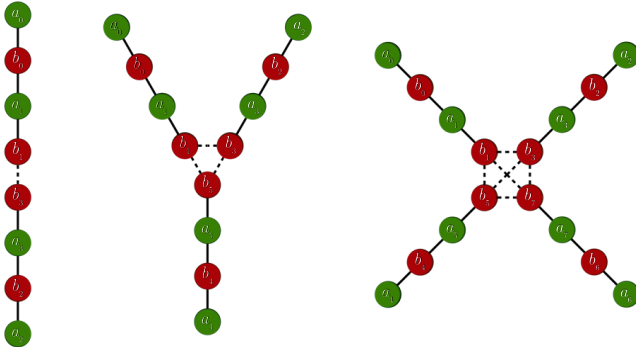


FIG. 7. Illustration of ordering of odd and even Majorana fermionic operators  $a_j$  and  $b_j$  for chains coupled in three scenarios; two chains, three chains in a Y-junction, and four chains in an X-junction. Sketches are for coupled chains of  $N = 4$  Majorana fermions each. We always ensure an even number of Majorana fermions in each chain.

operators, the Jordan-Wigner transformation can be formulated as

$$\begin{aligned} a_j &= K_j \sigma_j^x, \\ b_j &= K_j \sigma_j^y \\ &= -i K_{j+1} \sigma_j^x, \\ a_j b_j &= i \sigma_j^z, \end{aligned} \quad (\text{A2})$$

where in the second relation we used  $\sigma^y = -i\sigma^z\sigma^x$ . To map the interacting Kitaev chain to its dual spin model, we rewrite Eq. 1 in terms of  $a$  and  $b$  as well, such that

$$\begin{aligned} \mathcal{H} = \sum_j & iha_j b_j - iJb_j a_{j+1} - g_z a_j b_j a_{j+1} b_{j+1} \\ & - g_x b_j a_{j+1} b_{j+1} a_{j+2}, \end{aligned} \quad (\text{A3})$$

where the sum runs over all Majorana pairs. We renamed the constants  $t$  and  $g$  into their respective spin counterparts. We show a sketch of this relabeling in Fig.6. By applying the Jordan-Wigner transformation to the interacting Kitaev chain we find the spin Hamiltonian

$$\mathcal{H} = \sum_j J \sigma_j^x \sigma_{j+1}^x - h \sigma_j^z + g_z \sigma_j^z \sigma_{j+1}^z + g_x \sigma_j^x \sigma_{j+2}^x. \quad (\text{A4})$$

We always label the chains from the outer edges inward, which we illustrate for chains containing  $N = 4$  Majorana fermions each in Fig.7 for the three geometries considered in this study. This makes it so that, even for the benchmark case of coupling two chains, strings of  $\sigma_z$ -operators appear in the coupling term.

### The eigenvalue problem

To find the eigenvalues and eigenvectors we use the Lanczos algorithm [65]. This algorithm adopts power

methods to find the  $k$  smallest eigenvalues of a large symmetric sparse matrix - such as the Hamiltonians we consider in this study - by mapping the eigenvalue problem to one of a low-dimensional subspace. One, very effective, of such subspaces is that spanned by subsequently applying the Hamiltonian to the wavefunction - the Krylov basis.

This multiplication of a sparse matrix with a vector can be done without explicitly constructing the Hamiltonian itself, allowing studying larger systems. To formulate an implicit expression of the Hamiltonian we first look at what the Hamiltonian does to a single product state. Since a generic quantum state appears as a superposition of product states, let us illustrate what happens to this product state under the operators  $\sigma^x$  and  $\sigma^z$ . We represent a product state by a vector ones and zeros: one for spin up and zero for spin down. This string of ones and zeros is then stored as a binary number, and the different possible operations can be represented by binary operations. Applying  $\sigma_j^x$  to a state flips 0 to 1, or visa versa, at site  $j$  and  $\sigma_j^z$  multiplies the relative phase by  $-1$  when in the spin down configuration. The entangled state can then be represented as a vector, where the index is the product state and the value at that index is the relative phase. To illustrate this, we represent  $\frac{3}{5}|\uparrow\downarrow\rangle + \frac{4}{5}|\uparrow\uparrow\rangle$  as  $(0, 0, \frac{3}{5}, \frac{4}{5})^T$ , and applying  $\sigma_0^x \sigma_1^z$  to this vector results in  $(-\frac{3}{5}, \frac{4}{5}, 0, 0)^T$ . Then, by repeating this procedure for all terms in the Hamiltonian we apply the Hamiltonian to the wavefunction.

As an initial guess for the Lanczos algorithm we use wavefunction of the previous simulation, drastically reducing the number of iterations required for convergence. Note, for this we assume that eigenenergies of interest do not cross those that are not in our interest, i.e. a bulk state not studied before suddenly becomes part of the ground state spectrum.

To benchmark our implementation of the Lanczos algorithm and the coupling term  $\mathcal{H}_{\text{coupling}}(\alpha)$ , we run our algorithm for a junction with two chains each with 20 Majorana fermions and  $\alpha = 1$  and find a perfect agreement with previously reported zero modes in a single chain with 40 Majorana fermions [19].

### Appendix B: Additional results of X-junction

Besides the dependence on the magnetic field  $h$ , we also compute the dependence of the EZM on the interaction strength  $g$ . We show the logarithm of the ground state spectrum centered around its minimum in Fig.8 for  $h = 0.35$  and  $N = 10$  Majorana fermions on each chain. Once again, two states with opposite parity form a pair and show EZM. We also show the energy of these pairs centered around their mean in Fig.8(b). On top of that we also show the data for two coupled chains with  $N = 8$  Majorana fermions coupled by a strength  $\alpha = 2$ . Interestingly, and similar to the Y-junction, the chain closely matches the number and the location of the EZM to that

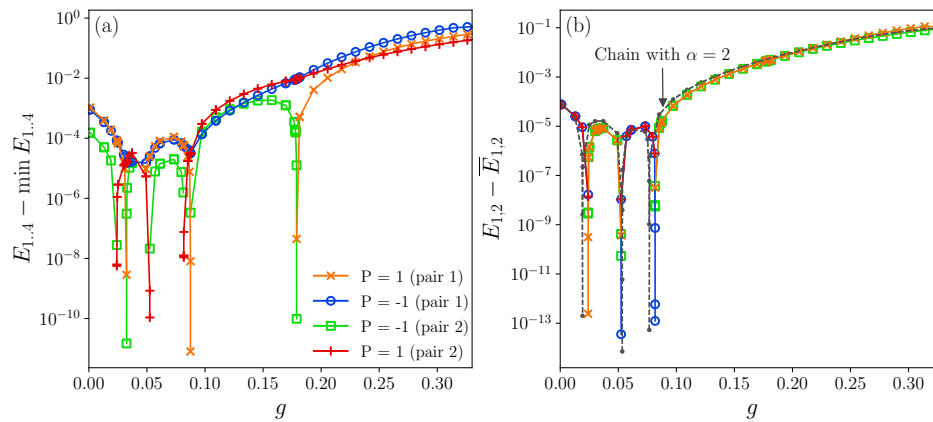


FIG. 8. Ground state spectrum of four chains coupled in the X-junction as a function of the interaction strength  $g$  in the chains. Data is shown for  $N = 8$  per chain and the magnetic field is fixed at  $h = 0.35$ . (a) Spectrum centered around the minimum of the four energies. States group into pairs with opposite parity. (b) Energy of the parity pairs centered around their respective mean. EZM of both pairs occur at the same location. Grey line shows the same but for two chains of  $N = 8$  Majorana fermions coupled by a strength  $\alpha = 2$ . The similarities between the X-junction and this chain are quite remarkable.

of the junction.

We once again observe that the difference within the

pairs of eigenvalues in the X-junction is similar to a chain with  $\alpha = 2$ , with the same amount of spin sites on each arm.

- 
- [1] C. Nayak, S. H. Simon, A. Stern, M. Freedman, and S. Das Sarma, Non-abelian anyons and topological quantum computation, *Rev. Mod. Phys.* **80**, 1083 (2008).
- [2] S. D. Sarma, M. Freedman, and C. Nayak, Majorana zero modes and topological quantum computation, *npj Quantum Inf* **1**, 10.1038/npjqi.2015.1 (2015).
- [3] P. Marra, Majorana nanowires for topological quantum computation, *Journal of Applied Physics* **132**, 231101 (2022).
- [4] A. Y. Kitaev, Unpaired Majorana fermions in quantum wires, *Physics-Uspekhi* **44**, 131 (2001).
- [5] P. Fendley, Parafermionic edge zero modes in Zn-invariant spin chains, *J. Stat. Mech.: Theor. Exp.* **2012**, P11020 (2012).
- [6] J. Alicea, New directions in the pursuit of Majorana fermions in solid state systems, *Rep. Prog. Phys.* **75**, 076501 (2012).
- [7] C. W. J. Beenakker, Search for Majorana Fermions in Superconductors, *Annual Review of Condensed Matter Physics* **4**, 113 (2013).
- [8] A. Das, Y. Ronen, Y. Most, Y. Oreg, M. Heiblum, and H. Shtrikman, Zero-bias peaks and splitting in an Al-InAs nanowire topological superconductor as a signature of Majorana fermions, *Nature Physics* **8**, 887 (2012).
- [9] M. T. Deng, C. L. Yu, G. Y. Huang, M. Larsson, P. Caroff, and H. Q. Xu, Anomalous Zero-Bias Conductance Peak in a Nb-InSb Nanowire-Nb Hybrid Device, *Nano Letters* **12**, 6414 (2012).
- [10] V. Mourik, K. Zuo, S. M. Frolov, S. R. Plissard, E. P. A. M. Bakkers, and L. P. Kouwenhoven, Signatures of Majorana Fermions in Hybrid Superconductor-Semiconductor Nanowire Devices, *Science* **336**, 1003 (2012).
- [11] L. P. Rokhinson, X. Liu, and J. K. Furdyna, The fractional a.c. Josephson effect in a semiconductor-superconductor nanowire as a signature of Majorana particles, *Nature Physics* **8**, 795 (2012).
- [12] R. Toskovic, R. van den Berg, A. Spinelli, I. S. Eliens, B. van den Toorn, B. Bryant, J.-S. Caux, and A. F. Otte, Atomic spin-chain realization of a model for quantum criticality, *Nature Phys* **12**, 656 (2016).
- [13] L. Fidkowski and A. Kitaev, Effects of interactions on the topological classification of free fermion systems, *Physical Review B* **81**, 134509 (2010).
- [14] L. Fidkowski and A. Kitaev, Topological phases of fermions in one dimension, *Physical Review B* **83**, 075103 (2011).
- [15] A. Rahmani, X. Zhu, M. Franz, and I. Affleck, Emergent Supersymmetry from Strongly Interacting Majorana Zero Modes, *Physical Review Letters* **115**, 166401 (2015).
- [16] A. Rahmani, X. Zhu, M. Franz, and I. Affleck, Phase diagram of the interacting Majorana chain model, *Phys. Rev. B* **92**, 235123 (2015).
- [17] H. Katsura, D. Schuricht, and M. Takahashi, Exact ground states and topological order in interacting Kitaev/Majorana chains, *Phys. Rev. B* **92**, 115137 (2015).
- [18] R. Verresen, A. Vishwanath, and F. Pollmann, Stable Luttinger liquids and emergent  $U(1)$  symmetry in constrained quantum chains, *arXiv: Strongly Correlated Electrons* (2019).
- [19] N. Chepiga and N. Laflorencie, Topological and quantum critical properties of the interacting Majorana chain model, *SciPost Phys.* **14**, 152 (2023).
- [20] E. Sela, A. Altland, and A. Rosch, Majorana fermions in strongly interacting helical liquids, *Phys. Rev. B* **84**, 085114 (2011).



- [21] N. Chepiga, Critical properties of the Majorana chain with competing interactions, *Phys. Rev. B* **108**, 054509 (2023).
- [22] N. Chepiga and F. Mila, Eight-vertex criticality in the interacting Kitaev chain, *Phys. Rev. B* **107**, L081106 (2023).
- [23] N. Laflorencie, Universal signatures of majorana zero modes in critical kitaev chains (2023), arXiv:2311.07571 [cond-mat.str-el].
- [24] F. Crépín, G. Zaránd, and P. Simon, Nonperturbative phase diagram of interacting disordered Majorana nanowires, *Phys. Rev. B* **90**, 121407 (2014).
- [25] N. M. Gergs, L. Fritz, and D. Schuricht, Topological order in the Kitaev/Majorana chain in the presence of disorder and interactions, *Phys. Rev. B* **93**, 075129 (2016).
- [26] J. F. Karcher, M. Sonner, and A. D. Mirlin, Disorder and interaction in chiral chains: Majoranas versus complex fermions, *Phys. Rev. B* **100**, 134207 (2019).
- [27] A. M. Lobos, R. M. Lutchyn, and S. Das Sarma, Interplay of Disorder and Interaction in Majorana Quantum Wires, *Phys. Rev. Lett.* **109**, 146403 (2012).
- [28] A. Milsted, L. Seabra, I. C. Fulga, C. W. J. Beenakker, and E. Cobanera, Statistical translation invariance protects a topological insulator from interactions, *Phys. Rev. B* **92**, 085139 (2015).
- [29] B. Roberts and O. I. Motrunich, Infinite randomness with continuously varying critical exponents in the random XYZ spin chain, *Phys. Rev. B* **104**, 214208 (2021).
- [30] N. Chepiga and N. Laflorencie, Resilient infinite randomness criticality for a disordered chain of interacting Majorana fermions, *Phys. Rev. Lett.* **132**, 056502 (2024).
- [31] J. A. Kjäll, J. H. Bardarson, and F. Pollmann, Many-Body Localization in a Disordered Quantum Ising Chain, *Phys. Rev. Lett.* **113**, 107204 (2014).
- [32] N. Laflorencie, G. Lemarié, and N. Macé, Topological order in random interacting Ising-Majorana chains stabilized by many-body localization, *Phys. Rev. Res.* **4**, L032016 (2022).
- [33] S. Moudgalya, D. A. Huse, and V. Khemani, Perturbative instability towards delocalization at phase transitions between MBL phases (2020), 2008.09113.
- [34] R. Sahay, F. Machado, B. Ye, C. R. Laumann, and N. Y. Yao, Emergent Ergodicity at the Transition between Many-Body Localized Phases, *Phys. Rev. Lett.* **126**, 100604 (2021).
- [35] T. B. Wahl, F. Venn, and B. Béri, Local integrals of motion detection of localization-protected topological order, *Phys. Rev. B* **105**, 144205 (2022).
- [36] G. Kells, Many-body Majorana operators and the equivalence of parity sectors, *Phys. Rev. B* **92**, 081401 (2015).
- [37] G. Kells, Multiparticle content of Majorana zero modes in the interacting  $\mathbb{Z}_2$ -wave wire, *Phys. Rev. B* **92**, 155434 (2015).
- [38] A. Więckowski, M. M. Maška, and M. Mierzejewski, Identification of Majorana Modes in Interacting Systems by Local Integrals of Motion, *Phys. Rev. Lett.* **120**, 040504 (2018).
- [39] T. Koma, Stability of Majorana Edge Zero Modes against Interactions (2022), 2205.11222 [math-ph].
- [40] P. Fendley, Strong zero modes and eigenstate phase transitions in the XYZ/interacting Majorana chain, *Journal of Physics A: Mathematical and Theoretical* **49**, 30LT01 (2016).
- [41] N. Chepiga and F. Mila, Exact zero modes in frustrated Haldane chains, *Phys. Rev. B* **96**, 060409 (2017).
- [42] G. Vionnet, B. Kumar, and F. Mila, Level crossings induced by a longitudinal coupling in the transverse field Ising chain, *Phys. Rev. B* **95**, 174404 (2017).
- [43] K. Wada, T. Sugimoto, and T. Tohyama, Coexistence of strong and weak Majorana zero modes in an anisotropic XY spin chain with second-neighbor interactions, *Phys. Rev. B* **104**, 075119 (2021).
- [44] A. Alexandradinata, N. Regnault, C. Fang, M. J. Gilbert, and B. A. Bernevig, Parafermionic phases with symmetry breaking and topological order, *Phys. Rev. B* **94**, 125103 (2016).
- [45] C.-Y. Hou and C. Chamon, Junctions of three quantum wires for spin-1/2 electrons, *Phys. Rev. B* **77**, 155422 (2008).
- [46] B. Bellazzini, P. Calabrese, and M. Mintchev, Junctions of anyonic luttinger wires, *Phys. Rev. B* **79**, 085122 (2009).
- [47] D. Giuliano and P. Sodano, Y-junction of superconducting josephson chains, *Nuclear Physics B* **811**, 395 (2009).
- [48] A. Rahmani, C.-Y. Hou, A. Feiguin, M. Oshikawa, C. Chamon, and I. Affleck, General method for calculating the universal conductance of strongly correlated junctions of multiple quantum wires, *Phys. Rev. B* **85**, 045120 (2012).
- [49] B. van Heck, A. R. Akhmerov, F. Hassler, M. Burrello, and C. W. J. Beenakker, Coulomb-assisted braiding of Majorana fermions in a Josephson junction array, *New J. Phys.* **14**, 035019 (2012).
- [50] T. E. Pahomi, M. Sigrist, and A. A. Soluyanov, Braiding Majorana corner modes in a second-order topological superconductor, *Phys. Rev. Research* **2**, 032068 (2020).
- [51] S.-B. Zhang, W. B. Rui, A. Calzona, S.-J. Choi, A. P. Schnyder, and B. Trauzettel, Topological and holonomic quantum computation based on second-order topological superconductors, *Phys. Rev. Research* **2**, 043025 (2020).
- [52] S. Ikegaya, W. B. Rui, D. Manske, and A. P. Schnyder, Tunable Majorana corner modes in noncentrosymmetric superconductors: Tunneling spectroscopy and edge imperfections, *Phys. Rev. Research* **3**, 023007 (2021).
- [53] Z. Yan, F. Song, and Z. Wang, Majorana Corner Modes in a High-Temperature Platform, *Phys. Rev. Lett.* **121**, 096803 (2018).
- [54] H. Guo and S. R. White, Density matrix renormalization group algorithms for y-junctions, *Phys. Rev. B* **74**, 060401 (2006).
- [55] F. Bucchieri, H. Babujian, V. E. Korepin, P. Sodano, and A. Trombettoni, Thermodynamics of the topological kondo model, *Nuclear Physics B* **896**, 52 (2015).
- [56] N. Chepiga and F. Mila, Excitation spectrum and density matrix renormalization group iterations, *Phys. Rev. B* **96**, 054425 (2017).
- [57] C. T. Olund, N. Y. Yao, and J. Kemp, Boundary strong zero modes, *Phys. Rev. B* **111**, L201114 (2025).
- [58] There are two consecutive crossing points located within the distance  $\delta h \approx 2 \cdot 10^{-3}$  for  $N = 10$ . This splitting vanishes fast with the system size, e.g. for  $N = 8$  the corresponding distance is twice as large. Compare with the X-junction in Fig.9(b) where the corresponding distance is  $O(10^{-1})$ .
- [59] J. Alicea, Y. Oreg, G. Refael, von Oppen. Felix, and M. P. A. Fisher, Non-Abelian statistics and topological quantum information processing in 1D wire networks, *Nature Phys* **7**, 412 (2011).

- [60] K. Flensberg, Non-Abelian Operations on Majorana Fermions via Single-Charge Control, *Phys. Rev. Lett.* **106**, 090503 (2011).
- [61] M. Hell, K. Flensberg, and M. Leijnse, Coupling and braiding Majorana bound states in networks defined in two-dimensional electron gases with proximity-induced superconductivity, *Phys. Rev. B* **96**, 035444 (2017).
- [62] T. Hyart, B. van Heck, I. C. Fulga, M. Burrello, A. R. Akhmerov, and C. W. J. Beenakker, Flux-controlled quantum computation with Majorana fermions, *Phys. Rev. B* **88**, 035121 (2013).
- [63] T. Karzig, A. Rahmani, F. von Oppen, and G. Refael, Optimal control of Majorana zero modes, *Phys. Rev. B* **91**, 201404 (2015).
- [64] S. Plugge, A. Rasmussen, R. Egger, and K. Flensberg, Majorana box qubits, *New J. Phys.* **19**, 012001 (2017).
- [65] C. Lanczos, An iteration method for the solution of the eigenvalue problem of linear differential and integral operators, *Journal of Research of the National Bureau of Standards* **45**, 255 (1950).